Large-Scale Dynamical Response to Differential Heating: Statistical Equilibrium States and Amplitude Vacillation

PHILIP D. THOMPSON

National Center for Atmospheric Research, Boulder CO 80307*

(Manuscript received 28 February 1986, in final form 17 November 1986)

ABSTRACT

This is a study of the statistical behavior of a very low order "general circulation model," consisting of a single finite-amplitude baroclinic wave interacting with a mean zonal shear flow, maintained against dissipation by differential heating. Starting with the equations for two-level quasi-geostrophic flow in a β-plane channel, we derive a closed system of evolution equations for five zonally-averaged quantities at 45° latitude—including net poleward heat transport, meridional kinetic energy and mean vertical shear (or mean horizontal temperature gradient).

This system of equations enables us to relate the equilibrium values of mean vertical shear between 250 and 750 mb and rms northward component of velocity at 500 mb to the rate of differential heating. The former is estimated to be 10.7 m s^{-1} at 45°S: Oort's observed statistics show that it is actually about 12 m s^{-1}. The theoretical estimate of the rms northward component of velocity at 45°S is 11.0 m s^{-1}. Oort's and Trenberth's statistics also give a value of about 11 m s^{-1}.

For conditions at 45°S during the Southern Hemisphere summer season, numerical integrations of our model equations show that amplitude vacillations around the equilibrium state have a period of about 22.7 days, which compares favorably with the observed periods reported by Webster and Keller in addition to Randel and Stanford. This is added confirmation that a very simple model may provide a physically valid basis for understanding the dominant large-scale dynamical response to differential heating.

1. Introduction

This work is concerned primarily with the interaction between a baroclinic wave and a mean zonal shear flow, maintained against dissipation by differential heating. The original purpose was simply to answer the following question: To what extent does the poleward heat transport associated with a single finite-amplitude baroclinic wave, whose wavelength corresponds to marginal instability in the linear sense, account for the observed average temperature gradient and eddy kinetic energy—for a realistic rate of differential heating?

Despite the narrowness of our aims, the simple physical model we have designed to study this question, its behavior and the way in which we have chosen to formulate it are all more or less closely related to the methods and results of earlier research in two different areas. Several aspects of the behavior of finite-amplitude baroclinic waves, for example, have been discussed by Pedlosky (1971), Pedlosky and Frenzen (1980), and Hart (1981), including vacillation, aperiodic and chaotic motions, and steady motion. Some phenomena due to wave resonance and wave interference have been treated by Loesch and Domaracki (1977) and Lindzen et al. (1982), respectively. These contributions, primarily analytical in approach, have been complemented by the numerical experiments of Smith and Reilly (1977) and Boville (1982). None of these studies, however, have dealt explicitly with flows that are driven by external heating: in fact, with the exception of Hart (1981), they say little about how the flow is maintained against dissipation. The latter process, of course, is an essential element in our present problem, and is treated explicitly.

Likewise, the model considered here has something in common with "zonally-averaged" general circulation models or climate models. Although it treats the flow as a superposition of a small number of modes in a spectral representation, we do not deal directly with the evolution equations for the modal amplitudes. Rather, we extract from the corresponding field equations an equivalent system of equations for zonally-averaged variables—such as average eddy kinetic energy, average temperature gradient and net poleward transport of heat. Thus, our model is, in some respects, similar to the truncated moment closure first proposed by Kurihara (1970) and later studied by Egger (1975). Schemes of the same general character, but differing in that the net poleward fluxes of heat and momentum are "parameterized," are discussed by Wiin-Nielsen and Fuenzalida (1975) and Ohring and Adler (1978). A more complete description of "zonally-averaged" models is given in the excellent and comprehensive review of Saltzman (1978).

* The National Center for Atmospheric Research is sponsored by the National Science Foundation.

In general, however, it would be more satisfactory to calculate the net heat transport explicitly, rather than "parameterize" it. Here we calculate heat transport directly, much as Held and Suarez (1978) have computed it from a low-order general circulation model. In this respect, our low order model might be regarded as a "maximally simplified" general circulation model with nonparameterized heat transport, in the spirit of Lorenz (1960).

The physical basis of this study is the two-level quasi-geostrophic model for flow in a β-plane channel, with differential heating and eddy diffusion of heat and momentum. The fluctuating velocity field is represented as the superposition of four sinusoidal modes, whose amplitudes determine the phases and amplitudes of a baroclinic wave at the two levels. Four pairs of those modes interact nonlinearly with a fifth mode, representing the average vertical shear. The thermodynamic energy and vorticity equations, when applied to this simple representation, then lead to a closed system of five evolution equations for the zonal averages of poleward heat transport, meridional kinetic energy, vertical shear, temperature variance and cross-correlation between temperature and geopotential. With externally prescribed differential heating, the evolution equations enable us to calculate those five statistical quantities as functions of time only.

It is noteworthy that our representation precludes net transfer of momentum. Although this shortcoming has a primary effect on the energy balance and the partition of kinetic energy between the mean zonal flow and the large-scale eddies, it appears to be of secondary importance in maintaining the heat balance. The poleward heat transport depends directly on vertical variations of wave-phase, whereas the meridional transport of momentum depends on north–south variations of phase. Differential momentum transport may induce heat transport indirectly by enhancing the mean vertical shear, but this effect is less direct than that of the heat transport on the mean temperature gradient (or vertical shear). We thus consider the vertical variations of phase to be more important than the north–south variations in producing the heat transport necessary to establish thermal equilibrium.

We first examine the system's behavior in the absence of dissipation and differential heating. If the average vertical shear is held fixed (i.e., if the effect of poleward heat transport on the average temperature gradient is removed), the stability properties of the finite-amplitude baroclinic wave are exactly the same as those for infinitesimal perturbations. If, however, the baroclinic wave and the mean vertical shear flow are fully coupled, the interactions become nonlinear and the system's behavior changes qualitatively: even in supercritical conditions, the wave does not grow indefinitely, but undergoes amplitude vacillations. This phenomenon arises from the fact that the nonlinear system has four invariants: in consequence, one can derive a first-order equation for the average vertical shear that has two "turning points," which not only implies periodicity but allows us to determine analytically the amplitude of vacillation.

The equations that include dissipation and differential heating can be solved analytically for the equilibrium (i.e., time-independent) values of all five statistical variables, for given values of heating rates. For reasonable values of heating and dissipation rates, our theoretical estimates of average vertical shear and average meridional kinetic energy are in very good agreement with the observed statistics of Oort (1983) and Trenberth (1982). Thus, the answer to our original question is that a single baroclinic wave, whose wavelength is that for marginal instability, transports about enough heat poleward to account for the pole-to-equator temperature difference and observed average eddy kinetic energy, particularly in the Southern Hemisphere.

To examine the way in which equilibrium is established, we have carried out a series of numerical integrations, in which the initial values of the statistical variables were their equilibrium values, corresponding to a particular rate of differential heating. That rate of heating was then increased impulsively at initial time, so that the system was initially out of balance. It was found that the system rapidly adjusts to the perturbed heating rate, but overshoots and undergoes amplitude vacillations. In general, their period is inversely proportional to the square root of the differential heating rate and directly proportional to the square root of the rate of dissipation. For plausible values of the rates of dissipation and differential heating, it appeared that the periods of vacillation might be expected to be 10–25 days.

This result was at first rather disturbing and cast some doubt on a simple model's ability to exhibit the main features of the thermal balance without introducing extraneous side effects: the frequency spectrum of net heat transport over a 10-year record of Northern Hemisphere data showed little evidence of vacillation. In the past year, however, Randel and Stanford (1985) have reported evidence of strong amplitude-vacillation with periods of 10–20 days, during three consecutive summer seasons *in the Southern Hemisphere.* It also came to my attention that an earlier paper (Webster and Keller, 1975) presents some indirect indication of amplitude-vacillation with periods of 18–23 days, also in the Southern Hemisphere. Evidently the effects of the topographical and thermal forcing due to the continents of the Northern Hemisphere are large enough to obscure the regularity of the heat transport associated with transient baroclinic waves. In any event, the existence of amplitude vacillation with periods in the predicted range now appears to support the essential validity of this simple model as a basis for understanding the large-scale dynamical response to differential heating.

2. Formulation of the model equations

The thermodynamic energy and vorticity equations for the two-level quasi-geostrophic model are well known and clearly derived in Holton (1972). They are

$$\frac{\partial}{\partial t}\nabla^2\psi + J(\psi, \nabla^2\psi) + J(\psi', \nabla^2\psi') + \beta\frac{\partial\psi}{\partial x} = \nu\nabla^2\nabla^2\psi \quad (1)$$

$$\frac{\partial}{\partial t}\nabla^2\psi' + J(\psi, \nabla^2\psi') + J(\psi', \nabla^2\psi) + \beta\frac{\partial\psi'}{\partial x} = \nu\nabla^2\nabla^2\psi' + \frac{2f\omega}{p_0} \quad (2)$$

$$\frac{\partial\psi'}{\partial t} + J(\psi, \psi') - \frac{\sigma p_0\omega}{4} = \nu\nabla^2\psi' + \frac{p_0 Q}{4f\rho\theta} \quad (3)$$

where the dependent variables ψ and ψ' are half the sum and difference of the geostrophic streamfunctions gz/f at 250 and 750 mb, respectively, and $\omega = dp/dt$ at 500 mb. The coordinate x is directed eastward along the length of a β-plane channel of width W, and y is directed northward. The operator ∇^2 is the horizontal Laplacian, and J is the horizontal Jacobian. The quantities treated as constants are ν, coefficient of eddy viscosity (here assumed to be the same as eddy heat conduction); β, northward derivative of the Coriolis parameter f; $p_0 = 1000$ mb; $\sigma = -(\partial\theta/\partial p)/f\rho\theta$; ρ and θ, standard values of density and potential temperature at 500 mb. The quantity Q is $d\theta/dt$ for the layer from 250 to 750 mb, here assumed to depend only on y and t.

It will simplify matters if we now eliminate ω between (2) and (3), with the result that:

$$\frac{\partial}{\partial t}(\nabla^2\psi' - k_r^2\psi') + J(\psi, \nabla^2\psi' - k_r^2\psi') + J(\psi', \nabla^2\psi) + \beta\frac{\partial\psi'}{\partial x} = \nu\nabla^2(\nabla^2\psi' - k_r^2\psi') - \frac{k_r^2 p_0}{4f\rho\theta}Q \quad (4)$$

in which $k_r^2 = 8f/\sigma p_0^2$ is the inverse square of the Rossby radius of deformation. If we regard Q as known or expressible in terms of ψ and ψ', (1) and (4) then comprise a complete system of equations in ψ and ψ'.

We next restrict ψ and ψ' to be of the form:

$$\psi(x, y, t) = \Psi(y, t) + \phi(x, y, t)$$
$$\psi'(x, y, t) = \Psi'(y, t) + \phi'(x, y, t) \quad (5)$$

where

$$\phi(x, y, t) = S(t)\sin\lambda x \sin\frac{\pi y}{W} + C(t)\cos\lambda x \sin\frac{\pi y}{W}$$

$$\phi'(x, y, t) = S'(t)\sin\lambda x \sin\frac{\pi y}{W} + C'(t)\cos\lambda x \sin\frac{\pi y}{W}. \quad (6)$$

An important property of ϕ and ϕ' is that

$$\nabla^2\phi = -k^2\phi; \quad \nabla^2\phi' = -k^2\phi' \quad (7)$$

for $k^2 = \lambda^2 + \pi^2/W^2$. The functional forms of Ψ and Ψ' will be specified later.

Substituting the expressions (5) into (1), we first observe that:

$$J(\psi, \nabla^2\psi) = \frac{\partial^3\Psi}{\partial y^3}\frac{\partial\phi}{\partial x} - \frac{\partial\Psi}{\partial y}\frac{\partial}{\partial x}\nabla^2\phi + J(\phi, \nabla^2\phi).$$

In view of (7), however, $J(\phi, \nabla^2\phi) = 0$ and

$$J(\psi, \nabla^2\psi) = -\left(\frac{\partial^2 U}{\partial y^2} + k^2 U\right)v$$

where $U = -\partial\Psi/\partial y$ and $v = \partial\phi/\partial x$. Similarly,

$$J(\psi', \nabla^2\psi') = -\left(\frac{\partial^2 U'}{\partial y^2} + k^2 U'\right)v'$$

in which $U' = -\partial\Psi'/\partial y$ and $v' = \partial\phi'/\partial x$. With these results, (1) reduces to

$$k^2\frac{\partial\phi}{\partial t} + \left(\frac{\partial^2 U}{\partial y^2} + k^2 U\right)v + \left(\frac{\partial^2 U'}{\partial y^2} + k^2 U'\right)v' - \beta v + \nu k^4\phi = -\frac{\partial}{\partial t}\left(\frac{\partial U}{\partial y}\right) + \nu\frac{\partial^2}{\partial y^2}\left(\frac{\partial U}{\partial y}\right) = F(y, t). \quad (8)$$

Turning to (4), we again invoke (7) to obtain

$$J(\psi, \nabla^2\psi') = -\frac{\partial^2 U'}{\partial y^2}v - k^2 Uv' - k^2 J(\phi, \phi')$$

$$J(\psi', \nabla^2\psi) = -\frac{\partial^2 U}{\partial y^2}v' - k^2 U'v + k^2 J(\phi, \phi'),$$

whence

$$J(\psi, \nabla^2\psi') + J(\psi', \nabla^2\psi) = -\left(\frac{\partial^2 U'}{\partial y^2} + k^2 U'\right)v - \left(\frac{\partial^2 U}{\partial y^2} + k^2 U\right)v'.$$

Moreover, from (5) and (6) we find that

$$J(\psi, \psi') = -U'v + Uv' + J(\phi, \phi')$$

$$J(\phi, \phi') = \frac{\pi\lambda}{W}(SC' - S'C)\sin\frac{\pi y}{W}\cos\frac{\pi y}{W}.$$

The important point to notice is that $J(\phi, \phi')$ depends only on y and t, and not on x. Introducing these results into (4), we arrive at

$$(k^2 + k_r^2)\frac{\partial\phi'}{\partial t} + \left(\frac{\partial^2 U}{\partial y^2} + k^2 U + k_r^2 U\right)v' + \left(\frac{\partial^2 U'}{\partial y^2} + k^2 U' - k_r^2 U'\right)v - \beta v' + \nu k^2(k^2 + k_r^2)\phi'$$
$$= \frac{\partial}{\partial t}\left(\frac{\partial^2\Psi'}{\partial y^2} - k_r^2\Psi'\right) - \nu\frac{\partial^2}{\partial y^2}\left(\frac{\partial^2\Psi'}{\partial y^2} - k_r^2\Psi'\right) - k_r^2 J(\phi, \phi') + \frac{k_r^2 p_0}{4f\rho\theta}Q(y, t) = F'(y, t). \quad (9)$$

Let us next consider the momentum budget for this model. In flux form, the eastward component of the equation of motion is

$$\frac{\partial u}{\partial t}+\frac{\partial}{\partial x}(uu)+\frac{\partial}{\partial y}(uv)+\frac{\partial}{\partial p}(u\omega)-fv+g\frac{\partial z}{\partial x}=\nu\nabla^2 u$$

where u and v are the eastward and northward components of velocity, respectively. Introducing the representation (5) into the equation above, averaging vertically with respect to p and averaging with respect to x over one full wavelength $2\pi/\lambda$, we find that

$$\frac{\partial U}{\partial t}-\frac{\partial}{\partial y}\left(\overline{\frac{\partial\phi}{\partial x}\frac{\partial\phi}{\partial y}}+\overline{\frac{\partial\phi'}{\partial x}\frac{\partial\phi'}{\partial y}}\right)=\nu\frac{\partial^2 U}{\partial y^2} \qquad (10)$$

where the x-average is denoted by the overbar. We note from (6), however, that

$$\overline{\frac{\partial\phi}{\partial x}\frac{\partial\phi}{\partial y}}=\frac{\pi\lambda}{W}CS\sin\frac{\pi y}{W}\cos\frac{\pi y}{W}\,\overline{\cos 2\lambda x}=0.$$

Similarly,

$$\overline{\frac{\partial\phi'}{\partial x}\frac{\partial\phi'}{\partial y}}=0.$$

Thus (10) reduces to

$$\frac{\partial U}{\partial t}=\nu\frac{\partial^2 U}{\partial y^2}.$$

A solution of this equation is clearly U = constant. We thus consider U, where it enters (8) and (9), as a constant of unspecified value. The value of that constant is immaterial, since U does not enter into the evolution equations for zonally-averaged quantities. This is simply a reflection of the fact that all information about absolute phase is lost in averaging: the relative phase, however, is preserved in U' and ϕ'.

Proceeding in much the same way, we may derive an evolution equation for U'. Introducing the representation (5) into the flux form of the thermodynamic energy equation, averaging vertically with respect to p and averaging with respect to x over one full wavelength $2\pi/\lambda$, we see that

$$\frac{\partial\Psi'}{\partial t}+\frac{\partial}{\partial y}\overline{v\phi'}=\nu\frac{\partial^2\Psi'}{\partial y^2}+\frac{p_0}{4f\rho\theta}Q(y)$$

or, differentiating with respect to y,

$$\frac{\partial U'}{\partial t}-\frac{\partial^2}{\partial y^2}\overline{v\phi'}=\nu\frac{\partial^2 U'}{\partial y^2}-\frac{p_0}{4f\rho\theta}\frac{\partial Q}{\partial y}. \qquad (11)$$

By direct calculation from (6), we find that

$$\overline{v\phi'}=\frac{\lambda}{2}(SC'-S'C)\sin^2\frac{\pi y}{W}, \qquad (12)$$

whence

$$\frac{\partial^2}{\partial y^2}\overline{v\phi'}=\frac{\pi^2\lambda}{W^2}(SC'-S'C)\left(\cos^2\frac{\pi y}{W}-\sin^2\frac{\pi y}{W}\right).$$

Thus, at $y = W/2$,

$$\frac{\partial^2}{\partial y^2}\overline{v\phi'}=-\frac{2\pi^2}{W^2}\overline{v\phi'}.$$

According to (12), the net poleward heat transport $\overline{v\phi'}$ attains its maximum value at $y = W/2$ and vanishes at $y = 0$ and $y = W$. We suppose that U', the mean zonal shear (or mean horizontal temperature gradient), behaves in the same way, so that at $y = W/2$:

$$\frac{\partial^2 U'}{\partial y^2}=-\frac{2\pi^2}{W^2}U'. \qquad (13)$$

With these results, (11) then reduces to

$$\frac{\partial U'}{\partial t}+\frac{2\pi^2}{W^2}\overline{v\phi'}=-\frac{2\pi^2\nu}{W^2}U'-\frac{p_0}{4f\rho\theta}\frac{\partial Q}{\partial y}. \qquad (14)$$

From here on, we shall apply (14) at $y = W/2$.

Two further equations, needed to complete the development, are obtained by differentiating (8) and (9) with respect to x, viz.,

$$\frac{\partial v}{\partial t}+U\frac{\partial v}{\partial x}+\frac{(k^2-k_w^2)}{k^2}U'\frac{\partial v'}{\partial x}-\frac{\beta}{k^2}\frac{\partial v}{\partial x}+\nu k^2 v=0 \qquad (15)$$

$$\frac{\partial v'}{\partial t}+U\frac{\partial v'}{\partial x}+\frac{(k^2-k_w^2-k_r^2)}{(k_r^2+k^2)}U'\frac{\partial v}{\partial x}-\frac{\beta}{k_r^2+k^2}\frac{\partial v'}{\partial x}+\nu k^2 v'=0 \qquad (16)$$

where $k_w^2 = 2\pi^2/W^2$.

Examining (14), we observe that the change in the mean vertical shear U' depends on the net poleward heat transport $\overline{v\phi'}$. The latter we predict from an equation for $\partial\overline{v\phi'}/\partial t$; this is found by multiplying (9) by $v/(k_r^2 + k^2)$, multiplying (15) by ϕ', adding those equations and averaging with respect to x over one full wavelength, with the result that

$$\frac{\partial}{\partial t}\overline{v\phi'}-\frac{(k_r^2+k_w^2-k^2)}{k_r^2+k^2}U'\overline{v^2}-\frac{(k^2-k_w^2)}{k^2}U'\overline{v'^2}+\frac{\beta k_r^2}{k^2(k_r^2+k^2)}\overline{vv'}+2\nu k^2\overline{v\phi'}=0. \qquad (17)$$

Equation (17) involves three other statistics—namely, $\overline{v^2}$, $\overline{v'^2}$, and $\overline{vv'}$. Multiplying (15) by v and averaging with respect to x, we find that

$$\frac{\partial}{\partial t}\overline{v^2}-\frac{2\lambda^2(k^2-k_w^2)}{k^2}U'\overline{v\phi'}+2\nu k^2\overline{v^2}=0. \qquad (18)$$

Similarly, multiplying (16) by v' and averaging with respect to x, we have

$$\frac{\partial}{\partial t}\overline{v'^2}-\frac{2\lambda^2(k_r^2+k_w^2-k^2)}{k_r^2+k^2}U'\overline{v\phi'}+2\nu k^2\overline{v'^2}=0. \qquad (19)$$

Finally, multiplying (15) by v', multiplying (16) by v, adding those equations and averaging with respect to x, we obtain

$$\frac{\partial}{\partial t}\overline{vv'} - \frac{\beta\lambda^2 k_r^2}{k^2(k_r^2+k^2)}\overline{v\phi'} + 2\nu k^2 \overline{vv'} = 0. \qquad (20)$$

Inspecting (14), (17), (18), (19) and (20), we note that they comprise a closed system of five equations involving the five variables U', $\overline{v\phi'}$, $\overline{v^2}$, $\overline{v'^2}$ and $\overline{vv'}$. The latter now depend only on t, since (14) and (17)–(20) apply at $y = W/2$. Our next concern is to study the behavior of solutions of this system, for specified differential heating $\partial Q/\partial y$.

3. Instability and amplitude vacillation

To simplify notation, we introduce the dimensionless variables K, V, X, T, S, τ and η, such that

$$\overline{v^2} = \frac{2\beta^2}{k^4}K, \quad \overline{v'^2} = \frac{2\beta^2 V}{k^4}, \quad \overline{vv'} = \frac{\beta^2}{k^4}X,$$

$$\overline{v\phi'} = \frac{\beta^2}{k^5}T, \quad U' = \frac{\beta}{k^2}S, \quad t = \frac{k\tau}{\beta}, \quad y = \frac{\eta}{k}.$$

Moreover, to place our results in a familiar setting, we suppose that k_r^2 is much greater than k_w^2—i.e., the radius of deformation is considerably less than W. Equations (14) and (17)–(20) then take the form

$$\frac{dT}{d\tau} - 2NSK - 2SV + RX + DT = 0 \qquad (21)$$

$$\frac{dK}{d\tau} - ST + DK = 0 \qquad (22)$$

$$\frac{dV}{d\tau} - NST + DV = 0 \qquad (23)$$

$$\frac{dX}{d\tau} - RT + DX = 0 \qquad (24)$$

$$\frac{dS}{d\tau} + 2LT + LDS + FH = 0 \qquad (25)$$

where the dimensionless constants N, R, D, L and F are given by

$$N = \frac{k_r^2 - k^2}{k_r^2 + k^2}, \quad R = \frac{k_r^2}{k_r^2 + k^2}, \quad D = \frac{2\nu k^3}{\beta}$$

$$L = \frac{\pi^2}{k^2 W^2}, \quad F = \frac{p_0 k^3}{4 f \beta \rho}.$$

The dimensionless rate of differential heating is

$$H = \frac{1}{\theta}\frac{\partial}{\partial \eta}\left(\frac{d\theta}{d\tau}\right).$$

In the remainder of this section, we discuss the behavior of the system in the absence of dissipation and differential heating, when $D = 0$ and $H = 0$. We first consider it from the standpoint of classical perturbation analysis, in which S is regarded as fixed. In this case, differentiating (21) with respect to τ and substituting for the time derivatives of K, V and X from (22)–(24), we arrive at a single equation in T, i.e.,

$$\frac{d^2 T}{d\tau^2} = (4NS^2 - R^2)T. \qquad (26)$$

Thus, the system is unstable if $S > \frac{1}{2}RN^{-1/2}$. The neutral curve in the (k, U') plane is determined by

$$4NS^2 - R^2 = 0$$

or, in terms of the dimensional variables,

$$k^8 - k_r^4 k^4 + \frac{\beta^2 k_r^4}{4U'^2} = 0.$$

Points on the neutral curve are then given by

$$k^4 = \frac{k_r^4}{2} \pm \left(\frac{k_r^8}{4} - \frac{\beta^2 k_r^4}{4U'^2}\right)^{1/2}.$$

The critical shear, below which the solutions are stable, is thus $U'_c = \beta/k_r^2$. The wavenumber for marginal instability is $k = 2^{-1/4}k_r$. These conclusions agree exactly with the results of perturbation analysis, but in this case apply to a wave of finite amplitude. The reason is simply that terms which are nonlinear in ϕ or ϕ' are missing from (8) and (9), owing to the fact that $\nabla^2\phi = -k^2\phi$ and $\nabla^2\phi' = -k^2\phi'$ for a wave with a *single* wavenumber k.

In all subsequent calculations k is taken to be the wavenumber for marginal linear instability—i.e., $k = 2^{-1/4}k_r$. With this value of k, $N = 0.1716$ and $R = 0.5858$.

For arbitrary but supercritical initial conditions, (26) implies that T exhibits exponential growth indefinitely, a fact that is directly traceable to the assumed decoupling of (25). We now consider the effect of the coupling of the mean vertical shear through the heat transport associated with the evolving baroclinic wave. In general, for $D = 0$ and $H = 0$, (21)–(25) reduce to

$$\frac{dT}{d\tau} = 2NSK + 2SV - RX \qquad (27)$$

$$\frac{dK}{d\tau} = ST \qquad (28)$$

$$\frac{dV}{d\tau} = NST \qquad (29)$$

$$\frac{dX}{d\tau} = RT \qquad (30)$$

$$\frac{dS}{d\tau} = -2LT. \qquad (31)$$

Since S is now considered variable, this system is nonlinear. It does, however, possess four independent invariants. (It obviously cannot have more than four!) For example, multiplying (30) by $2L$, multiplying (31) by R, and adding those equations, we see that:

$$\frac{d}{d\tau}(2LX+RS)=0. \tag{32}$$

Similarly, multiplying (28) by $2L$, multiplying (31) by S and adding, we obtain

$$\frac{d}{d\tau}\left(2LK+\frac{1}{2}S^2\right)=0. \tag{33}$$

In much the same way we find that:

$$\frac{d}{d\tau}\left(2LV+\frac{N}{2}S^2\right)=0. \tag{34}$$

Finally, we multiply (27) by T, multiply (28) by $-2NK$, multiply (29) by $-2V/N$, multiply (30) by X and add those four equations, with the result that

$$\frac{d}{d\tau}\left(\frac{1}{2}T^2-NK^2-\frac{1}{N}V^2+\frac{1}{2}X^2\right)=0. \tag{35}$$

Equations (32)–(35) enable us to express X, K, V and T in terms of S, since they clearly imply that

$$X=X_0-\frac{R}{2L}(S-S_0) \quad K=K_0-\frac{1}{4L}(S^2-S_0^2)$$

$$V=V_0-\frac{N}{4L}(S^2-S_0^2)$$

$$T^2=T_0^2+(X_0^2-X^2)-2N(K_0^2-K^2)-\frac{2}{N}(V_0^2-V^2) \tag{36}$$

where the subscript zero denotes an initial value. Thus, substituting for X, K and V in (36), we may express T^2 in terms of S. Then (31) takes the form:

$$\frac{dS}{d\tau}=\mp 2L\left\{X_0^2-\left[X_0-\frac{R}{2L}(S-S_0)\right]^2-2NK_0^2 + 2N\left[K_0-\frac{1}{4L}(S^2-S_0^2)\right]^2-\frac{2}{N}V_0^2 + \frac{2}{N}\left[V_0-\frac{N}{4L}(S^2-S_0^2)\right]^2+T_0^2\right\}^{1/2}. \tag{37}$$

We observe that this equation involves only one variable, S. The quantity in braces is a polynomial of fourth degree in S, which may vanish for two, four or no real values of S. Call it $P(S)$. Its value for $S=S_0$ is just T_0^2 and thus is positive. At initial time, we clearly choose the negative sign of the radical.

Initially the radical is real and must remain so. Thus, imagining that we are integrating (37) forward in time, we see that S decreases (or increases) monotonically until it reaches a real root of $P(S)=0$. At that point, we reverse the sign of the radical, since $dS/d\tau$ cannot be imaginary. The solution S of (37) thus oscillates periodically between two real roots of $P(S)=0$, bracketing S_0. The variables T, K, V and X exhibit corresponding periodic oscillations, since they are all functions of S. This behavior is amplitude vacillation.

The properties of solutions of (37) are exactly analogous to those of the first-order equation for $x=\sin kt$, namely:

$$\frac{dx}{dt}=\pm k(1-x^2)^{1/2}, \quad x(0)=0.$$

Initially we choose the positive sign of the radical: x then increases until it reaches unity (one real root of the polynomial radicand), when dx/dt reverses sign. It then decreases until it reaches minus one (the other real root of the radicand), when dx/dt again reverses sign, and so on.

The rather striking qualitative change in behavior of the system, with and without the two-way interaction between the baroclinic wave and the mean zonal shear flow, is illustrated in Figs. 1 and 2. Figure 1 shows the net meridional heat transport, meridional kinetic energy and mean zonal wind shear plotted against number of time steps. These curves were constructed by integrating (27)–(30) numerically, with S held at a *fixed* value of 0.75. Figure 2 shows the curves constructed by integrating (27)–(31) numerically, for $S_0=0.75$. The two calculations were identical in all other respects, so that they differ only in that S is coupled in the second calculation, but not in the first.

The system is slightly supercritical (in the linear sense) for $S=0.75$. As expected, therefore, Fig. 1 shows a continued exponential increase of heat transport and meridional kinetic energy. Figure 2, on the other hand, shows that kinetic energy reaches a maximum at about 1480 time steps, and subsequently decreases to its initial value. At the same time, the mean zonal shear decreases to a minimum of about 0.62 at around 1480 time steps, and then rises to its initial value. The latter result is in good agreement with (37): for $T_0=0$, $K_0=0.10$, $V_0=0$, $X_0=0$, $S_0=0.75$, two adjacent real roots of $P(S)=0$ are 0.75 and approximately 0.62, so that S oscillates between those two values.

4. Statistical equilibrium state

Let us next consider stationary solutions of (21)–(25) for $D\neq 0$ and nonzero time-independent values of H. They are solutions of the system:

$$-2NSK-2SV+RX+DT=0 \tag{38}$$

$$DK=ST \tag{39}$$

$$DV=NST \tag{40}$$

$$DX=RT \tag{41}$$

$$2LT+LDS+FH=0. \tag{42}$$

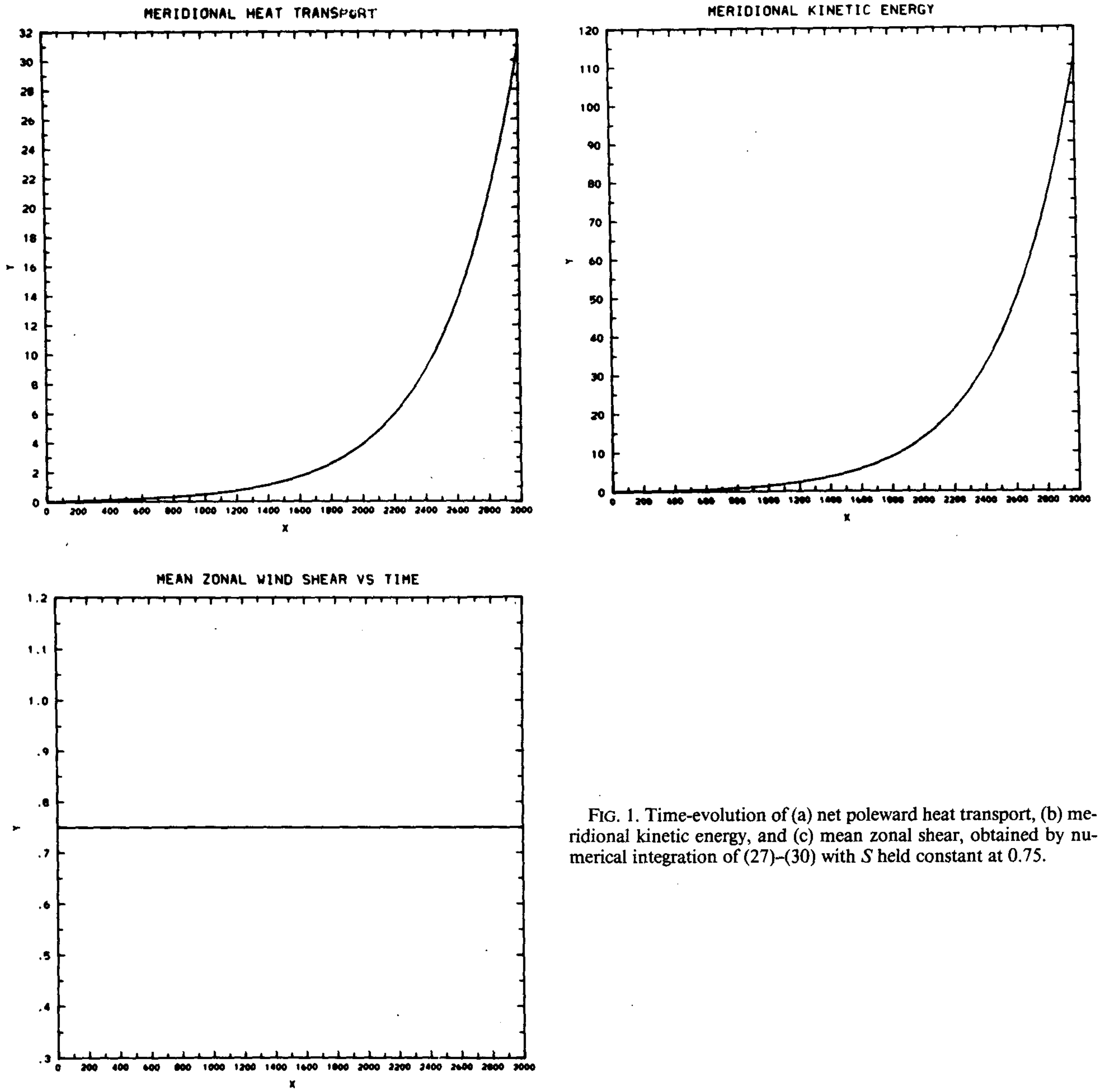

FIG. 1. Time-evolution of (a) net poleward heat transport, (b) meridional kinetic energy, and (c) mean zonal shear, obtained by numerical integration of (27)–(30) with S held constant at 0.75.

Solving (39), (40) and (41) for K, V and X and substituting for K, V and X in (38), we find that

$$S=\frac{1}{2}\left(\frac{R^2+D^2}{N}\right)^{1/2}. \tag{43}$$

We observe that, for small D, the stationary value of S approaches the critical value for linear instability: for realistic values of D, it is not much greater.

Taking into account the scaling of S, we infer that the mean vertical shear U' is proportional to $\partial\theta/\partial p$ by a very nearly constant factor: consequently, the slope of the average isentropic surfaces is approximately constant, independent of the differential heating. An increase in the mean horizontal temperature gradient is evidently accompanied by an increase in static stability, and conversely.

Let us next apply (43) to estimate the mean vertical shear at 45° latitude in the Southern Hemisphere, where the approximations of our model are most nearly valid. To do so, we identify conditions at $y = W/2$ in the model with real conditions at 45°S. For $D = 0.202$ (corresponding to an e-folding time of 6.5 days), (43) gives an equilibrium value of S equal to 0.748. This result is not very sensitive to variations of D, since D is appreciably less than R.

To attach the appropriate units to S we must estimate k_r, which depends on f, ρ, θ and $\partial\theta/\partial p$. The value of f

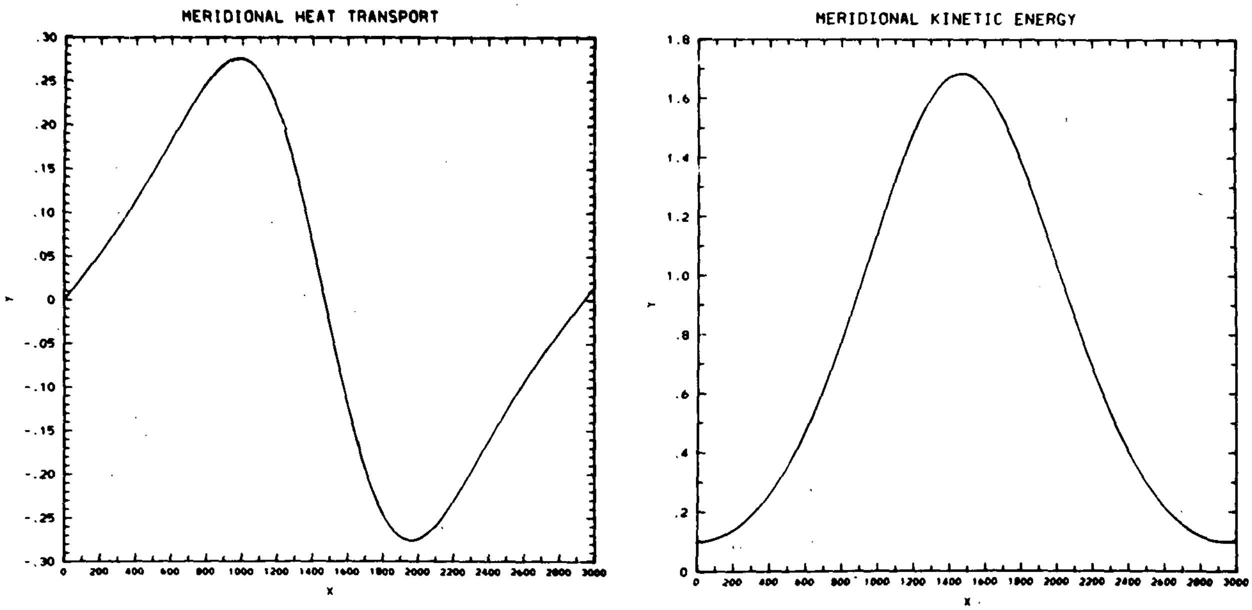

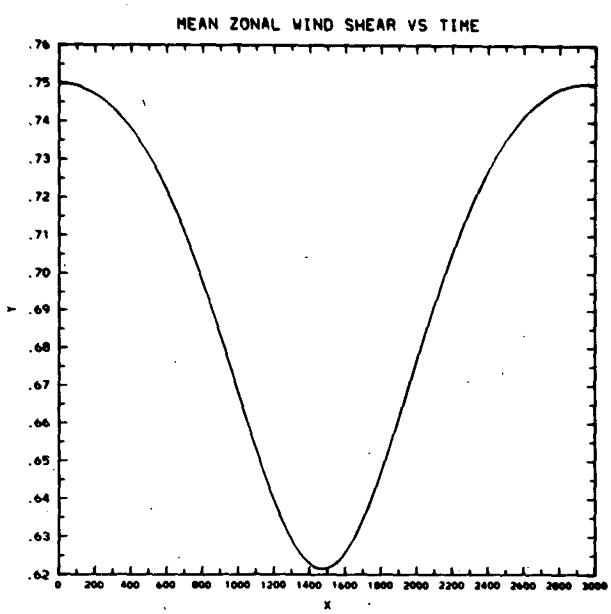

FIG. 2. As in Fig. 1, and obtained by numerical integration from the same initial conditions, but with S varying according to (31). Note that the scale of the ordinate is not the same as in Fig. 1.

is that at 45°S: the values of ρ, θ and $\partial\theta/\partial p$ for the layer from 250 to 750 mb were calculated from Oort's (1983) statistics for 45°S. The value of k_r estimated from these figures is 0.00146 km^{-1}, and is about the same for both the summer and winter seasons. Together with the value of β for 45°S, this value of k_r yields the appropriate unit of speed, which is 7.15 m s^{-1}. Hence, the *dimensional* value of the equilibrium mean vertical shear is

$$U' = 0.748 \times 7.15 \text{ m s}^{-1}$$
$$= 5.35 \text{ m s}^{-1}.$$

Since the difference between the mean zonal wind speeds at 250 and 750 mb was defined as *twice* U', that difference is 10.7 m s^{-1}. Oort's (1983) statistics for 45°S show that this difference is actually about 12 m s^{-1} during the summer season and is only slightly greater during the winter. This result, of course, also implies that the theoretical estimate of mean horizontal temperature gradient at 45°S is approximately correct.

With the equilibrium value of S and a specified rate of differential heating, (42) enables us to calculate the equilibrium heat transport. There are, of course, considerable uncertainties in estimating heating rates, particularly in the Southern Hemisphere. Our estimates were obtained by forming vertical, zonal and time averages of the heating rates calculated by Kasahara, Mizzi and Mohanty for 27 January to 10 February

1979. The difference between the average heating rates at 30° and 60°S was found to be about 0.61°K day^{-1}. With our present scaling, that rate of differential heating corresponds to $-FH = 0.051$. Thus, taking $D = 0.202$, $L = 0.065$ ($W = 10000$ km), and the equilibrium value of the mean shear $S = 0.748$, (42) yields an equilibrium heat transport T equal to 0.322. Introducing that value of T and $S = 0.748$ into (39), we find that the equilibrium *meridional* kinetic energy is 1.19. The corresponding dimensionless rms value of v is 1.54 or, with our present scaling, 11.0 m s^{-1}. According to Oort (1983) and Trenberth (1982), the observed standard deviation of v at 500 mb and 45°S during the Southern Hemisphere summer season is just about 11 m s^{-1}. (See cross-section SDV, DJF on p. 161 of Oort. The reader is assured that the constants that enter in this calculation were fixed and the calculation was completed *before* I saw Oort's rms values of v.) In that region the actual average value of v is very small, so that the rms value of v in our model may be compared with the standard deviation of v in the atmosphere. The closeness of agreement must be fortuitous, in view of the simplifications of our model, β-plane geometry, and uncertainties of the rate of differential heating: moreover, in our model all of the eddy kinetic energy is concentrated in a single narrow spectral band, whereas Oort's statistics embrace motions over a broad range of scales. Considering other points of agreement, however, one would conclude that our simple model appears to reflect the dominant features of the large-scale dynamical response to differential heating.

5. Amplitude vacillation around equilibrium

To see how rapidly the system adjusts to changes of differential heating and to study the nature of its transient response, we have carried out two series of numerical experiments for different rates of differential heating and dissipation, and for different departures from equilibrium. In each experiment, we integrated (21)–(25) by a predictor–corrector method in time steps of 0.01 units of dimensionless time. In all experiments, $N = 0.1716$, $R = 0.5858$ and $L = 0.065$. In each of the two series, we carried out numerical integrations of (21)–(25) for $D = 0.101$, 0.202 and 0.404 and for $-FH = 0.05$, 0.10, 0.20, 0.40 and 0.80, making 15 integrations in each series.

The initial values of T, K, V, X and S for each integration were just their equilibrium values for a particular value of $-FH$. That value of $-FH$ was then impulsively increased at initial time, by 5 percent in one series of experiments and by 10 percent in the other. Thus, in each experiment, the system is out of balance initially, and the question is how it evolves subsequently.

An example of the equilibration and transient response is shown in Fig. 3, which displays T, K and S as functions of time for $D = 0.202$ and $-FH = 0.051$. These values, as well as all other constants, are exactly those from which the equilibrium values of S and K were calculated in section 4 and most nearly characterize real conditions at 45°S during the Southern Hemisphere summer. In this case, an impulsive increase of $-FH$ by 10 percent produces vacillations around the new equilibrium state, with amplitudes about 5 percent of the equilibrium values. The period of the vacillation is about 1750 time steps of 0.01 units. With our present scaling, the unit of time is 1.30 days, so that the period of the vacillation is about 22.7 days. This estimate is to be compared with the vacillation periods of 18–23 days reported by Webster and Keller (1975) and the vacillation periods of 10–20 days described by Randel and Stanford (1985), for the summer seasons of 1978/79, 1979/80 and 1980/81 in the Southern Hemisphere.

The way in which the period of vacillation depends on the rates of dissipation and differential heating is summarized in Figs. 4(a) and 4(b). These show isopleths of the logarithm of the period for intervals of 0.1, as determined by numerical integration of (21)–(25), as a function of $\log D$ and $\log(-FH)$. It is striking that the isopleths are very nearly straight lines, parallel and equally-spaced. We note, moreover, that the logarithm of the period decreases by about 0.5 as $\log(-FH)$ increases by 1.0. Thus, since the isopleths have a slope of about unity, the period of vacillation appears to vary as the square root of D and inversely as the square root of $-FH$.

Figures 4a and 4b give the results for two series of experiments in which the rate of differential heating was impulsively increased by 5 or by 10 percent, respectively. Changing the magnitude of the impulsive increase is thus seen to have little effect on the period of vacillation: it does, however, have the expected effect of changing the amplitude of vacillation by a proportional amount.

6. Summary and conclusions

Our main concern has been to see to what extent the interaction between a single finite-amplitude baroclinic wave and a mean zonal shear flow accounts for the observed mean temperature gradient and mean eddy kinetic energy, for realistic rates of dissipation and differential heating. To study this question, we have represented the fluctuating part of the flow as a superposition of four sinusoidal modes whose amplitudes determine the phases and amplitudes of a baroclinic wave at two levels: all four modes have the same wavenumber, later chosen to correspond to marginal instability in the linear sense. Four pairs of those modes interact nonlinearly with a fifth mode, representing the mean zonal shear flow.

This representation is substituted into the equations for two-level quasi-geostrophic flow in a β-plane channel, not with a view to deriving evolution equations

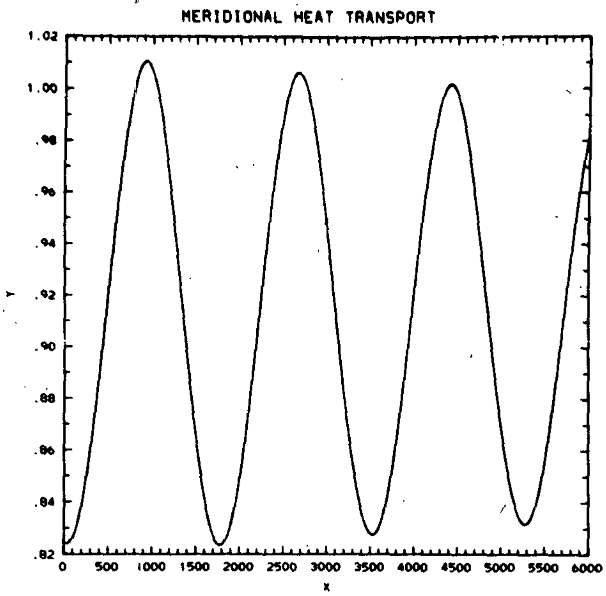

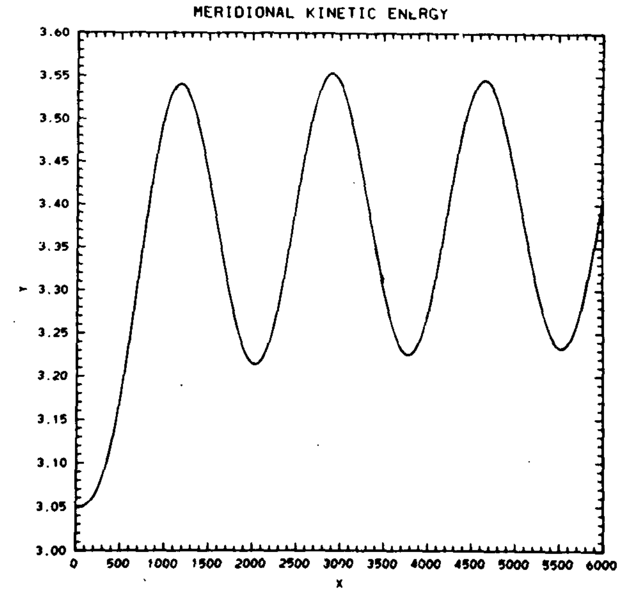

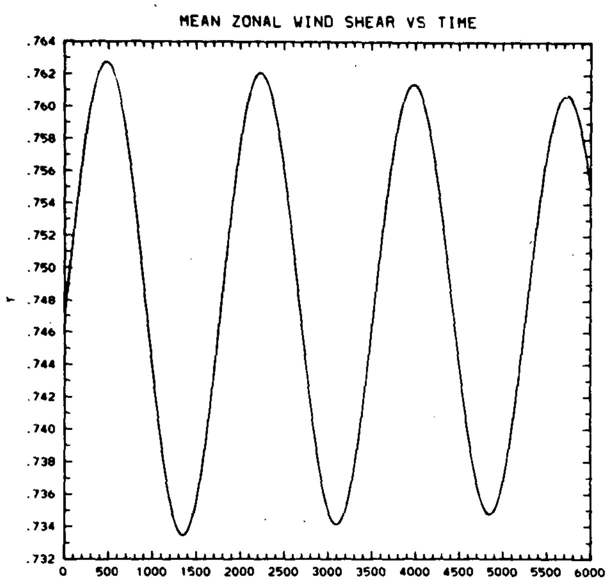

FIG. 3. Amplitude-vacillations of (a) net poleward heat transport, (b) meridional kinetic energy and (c) mean zonal shear. All variables were initially in equilibrium for a particular rate of differential heating. The latter was increased impulsively by 10 percent at initial time. In adjusting to new external conditions, the system vacillates around a new "equilibrium" state, but does not rapidly attain it.

for the modal amplitudes, but to extract a closed system of equations for five zonally-averaged statistics. They are: net poleward heat transport, mean meridional kinetic energy, temperature variance, cross-correlation between temperature and geopotential, and mean vertical wind shear. Those equations are nonlinear and fully coupled. With externally prescribed differential heating, they describe the model's statistical–dynamical response.

As a preliminary to numerical experiments with the general, time-dependent form of the model equations, we have examined the behavior of solutions in the absence of heating and dissipation. If the mean vertical shear is held fixed (i.e., uncoupled from the dynamical system), the solutions have the same stability properties as those in a linear system, but for finite amplitude. If, however, the mean vertical shear is fully coupled, the system undergoes a qualitative change in character: even in supercritical conditions, the solutions do not amplify indefinitely, but are bounded and periodic. This behavior, which owes its existence to the invariance of four independent functions of the variables, is amplitude vacillation in its pure form. The amplitude of vacillation is shown to be fixed by the real roots of a quartic polynomial and depends on the initial conditions.

The "steady-state" form of the equations is a system of nonlinear algebraic equations that can be readily solved for the equilibrium values of the five statistical variables. Using values of coefficients based on Oort's

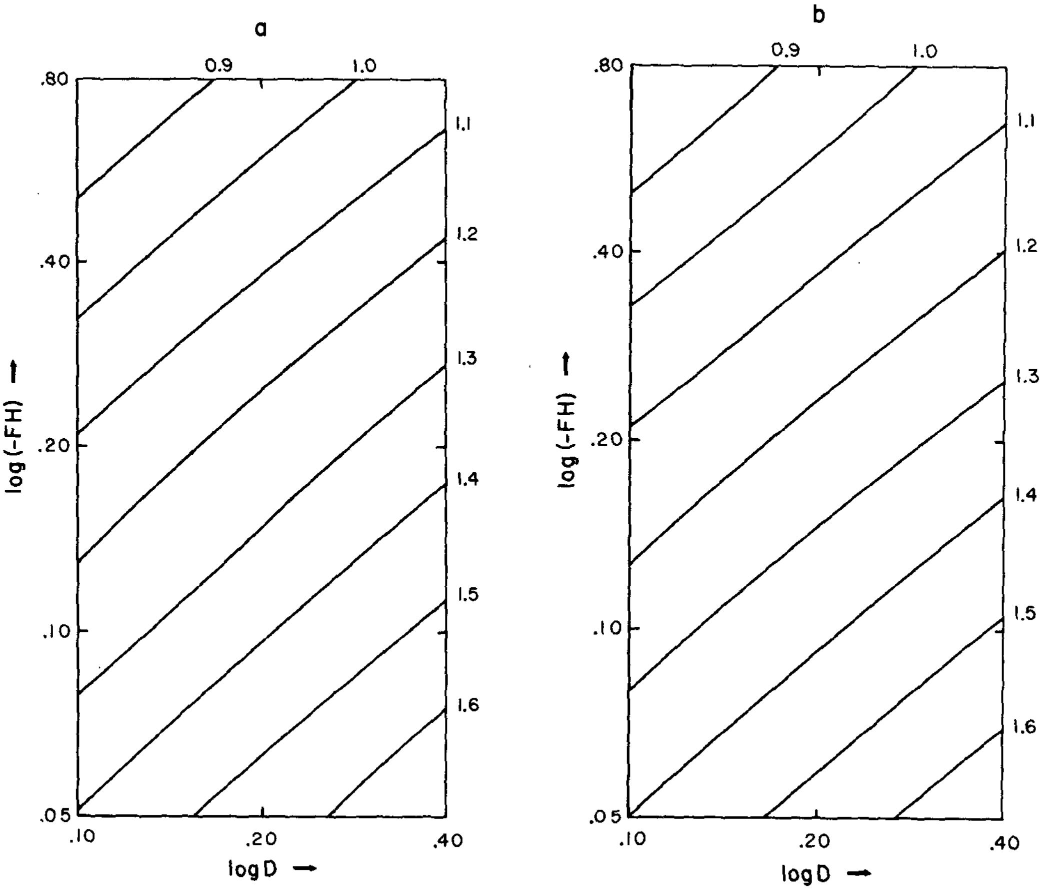

FIG. 4. Logarithm of vacillation period as a function of log$D$ and log($-FH$) for (a) rate of differential heating increased impulsively by 5 percent at initial time and (b) increased by 10 percent at initial time.

(1983) statistics at 45°S, we have estimated the mean vertical shear between 250 and 750 mb at 45°S, where the approximations of the model are most nearly valid. For a "dissipation" time of 6.5 days, the theoretical estimate of the mean vertical shear is 10.7 m s^{-1}: the observed mean shear, as reported by Oort (1983), is about 12 m s^{-1}. Moreover, with a differential heating rate derived from the recent calculations of Kasahara, Mizzi and Mohanty, the theoretical estimate of the rms northward component of velocity at 500 mb and 45°S is 11.0 m s^{-1}: by some (no doubt fortuitous) circumstance, Oort's (1983) and Trenberth's (1982) observed rms value is also about 11 m s^{-1}. Thus, in at least some important respects, the statistics of our simple model agree very well with the observed statistics of the Southern Hemisphere circulation. Since such quantities as mean zonal shear, net poleward heat transport, and meridional kinetic energy are all small at pole and equator and reach pronounced maxima near 45°S, their values at 45°S fairly well characterize the major statistical features of the tropospheric flow.

Finally, by carrying out a series of numerical integrations of the general, time-dependent model equations for different rates of dissipation and differential heating, we find that the period of amplitude-vacillation around an equilibrium state is proportional to the square root of the dissipation rate, and inversely proportional to the square root of the rate of differential heating. With the same coefficients as those used to estimate equilibrium values, the period of vacillation at 45°S during the Southern Hemisphere summer is estimated to be about 22.7 days. This figure compares favorably with the observed vacillation periods of 18–23 days reported by Webster and Keller (1975) and the periods of 10–20 days reported by Randel and Stanford (1985). This agreement appears to be added confirmation of the validity of our simple model as a physical basis for a general understanding of the dominant large-scale dynamical response to differential heating.

As indicated in the Introduction, our theoretical results (not surprisingly) appear to agree best with the observed structure and behavior of the large-scale flow in the Southern Hemisphere. In the Northern Hemisphere, the thermal and topographical forcing by large continents produces strong zonal asymmetries that tend to localize baroclinic eddies in "storm track" regions. In the Southern Hemisphere, however, the forcing is more nearly zonally symmetric, and complete trains of uniform baroclinic waves are often observed to girdle the whole hemisphere. Only under such circumstances would one expect to observe regular vacillation cycles and a simple dependence of heat transport on mean horizontal temperature gradient and differential heating.

Considering the approximations of our simple model, β-plane geometry and uncertainties about heating and dissipation rates, the agreement between our theoretical estimates and the observed statistical structure of the large-scale flow is gratifyingly close, but not entirely for the right reasons. We thus conclude that the *closeness* of agreement must be fortuitous. In view of several different points of qualitative and at least semiquantitative agreement, however, we might also conclude that the most important dynamical elements of the heat balance are contained in our model.

Encouraging as these results may be, one should not lose sight of the shortcomings inherent in such a simple model. Quite apart from its lack of resolution, some mechanisms that are important in maintaining the momentum and water balance are completely missing from the model, as are details of the processes of heating. At most, then, this model can only reflect the dominant effects in maintaining the thermal balance with zonally-averaged differential heating, whatever its origin.

Nevertheless, models of this type and low degree of complexity appear to have a proper place in the study of climate. Owing to the tremendous volume of computation required for integration of the complete equations, high-resolution general circulation models are not particularly well-suited to the study of climate dynamics on time scales of centuries or decades, or even years. Whatever other virtues low-order models may lack, they at least have the advantage of speed and simplicity, permitting rapid exploration of multiparameter domains and calculation of sizeable ensembles of solutions. With differential heating rates coupled to the model's dynamical and thermodynamical state, the simple model considered here may yield useful first-order estimates of the effects of "feedback" between the model's internal dynamics and various heating processes that are modulated by atmospheric conditions. In this respect, such models may serve as guides in designing and interpreting numerical experiments with more complicated models.

Acknowledgments. I wish to recognize Arthur Mizzi's able assistance in carrying out the numerical integrations described in sections 3 and 5, and to thank Mary Niemczewski for deciphering my handwriting and typing the manuscript.

REFERENCES

Boville, B., 1982: Strongly nonlinear vacillations in baroclinic waves. *J. Atmos. Sci.*, **39**, 1227–1240.

Egger, J., 1975: A statistical–dynamical model of the zonally averaged steady-state of the general circulation of the atmosphere. *Tellus*, **27**, 325–350.

Hart, J. E., 1981: Wavenumber selection in nonlinear baroclinic instability. *J. Atmos. Sci.*, **38**, 400–408.

Held, I. M., and M. J. Suarez, 1978: A two-level primitive equation atmospheric model designed for climatic sensitivity experiments. *J. Atmos. Sci.*, **35**, 206–229.

Holton, J., 1972: *An Introduction to Dynamic Meteorology.* Academic Press, 319 pp.

Kasahara, A., A. Mizzi and U. C. Mohanty, 1986: Evaluation of global diabatic heating rate from FGGE Level IIIb analyses and satellite radiation imagery data. Submitted for publication in *Mon. Wea. Rev.*

Kurihara, Y., 1970: A statistical–dynamical model of the general circulation of the atmosphere. *J. Atmos. Sci.*, **27**, 847–870.

Lindzen, R. S., B. Farrell and D. Jacqmin, 1982: Vacillations due to wave interference: Applications to the atmosphere and to annulus experiments. *J. Atmos. Sci.*, **39**, 14–23.

Loesch, A. Z., and A. Domaracki, 1977: Dynamics of N resonantly interacting baroclinic waves. *J. Atmos. Sci.*, **34**, 22–35.

Lorenz, E. N., 1960: Maximum simplification of the dynamic equations. *Tellus*, **12**, 243–254.

Ohring, G., and S. Adler, 1978: Some experiments with a zonally averaged climate model. *J. Atmos. Sci.*, **35**, 186–205.

Oort, A. H., 1983: Global atmospheric circulation statistics, 1958–1973. *NOAA* Prof. Paper 14, Rockville, MD.

Pedlosky, J., 1971: Finite-amplitude baroclinic waves with small dissipation. *J. Atmos. Sci.*, **28**, 587–597.

——, and C. Frenzen, 1980: Chaotic and periodic behavior of finite-amplitude baroclinic waves. *J. Atmos. Sci.*, **37**, 1177–1196.

Randel, W. J., and J. L. Stanford, 1985: An observational study of medium-scale wave dynamics in the Southern Hemisphere summer. Part I: Wave structure and energetics. *J. Atmos. Sci.*, **42**, 1172–1188.

Saltzman, B., 1978: A survey of statistical-dynamical models of the terrestrial climate. *Advances in Geophysics*, Vol 20, Academic Press, 184–304.

Smith, R. K., and J. M. Reilly, 1977: On a theory of amplitude vacillation in baroclinic waves: some numerical solutions. *J. Atmos. Sci.*, **34**, 1256–1260.

Trenberth, K. E., 1982: Seasonality in southern hemisphere eddy statistics at 500 mb. *J. Atmos. Sci.*, **39**, 2507–2520.

Webster, P., and J. L. Keller, 1975: Atmospheric variations: vacillations and index cycles. *J. Atmos. Sci.*, **32**, 1283–1300.

Wiin-Nielsen, A. C., and H. Fuenzalida, 1975: On the simulation of the axisymmetric circulation of the atmosphere. *Tellus*, **27**, 199–214.